Advanced Studies in Biology, Vol. 10, 2018, no. 1, 45 - 59
HIKARI Ltd, www.m-hikari.com
https://doi.org/10.12988/asb.2018.846

Non-Uniform Channels Mixing and Template Matching Based Denoising of Retinal Images for Optic Disk Detection

Khan Bahadar Khan*

Department of Telecommunication Engineering, UCET
The Islamia University of Bahawalpur, Pakistan
* Corresponding author

Naeem Iqbal Ratyal

Department of Electrical Engineering
Mirpur University of Science and Technology, Mirpur Azad Kashmir, Pakistan

Ali Sufyan

Department of Telecommunication Engineering, UCET
The Islamia University of Bahawalpur, Pakistan

M. R. Anjum

Department of Electronic Engineering, UCET
The Islamia University of Bahawalpur, Pakistan

Muhammad Shahid

The Istituto Italiano di Tecnologia – IIT
PAVIS - Pattern Analysis and Computer Vision Lab, Italy

Abstract

Optic Disc (OD) recognition is a fundamental phase in the developing methods for automated analysis of different chronic ocular disorders. In this article, a novel

technique has been introduced for OD detection and borderline extraction, which can be witnessed as a milestone in the advancement of a Computer-Assisted Diagnostic (CAD) framework for glaucoma detection in fundus photographs. A unique solution has been presented for removal of illuminated light spots due to refraction of camera light (so called fringe noise) on the edges of the retinal color images, which leads to false detection of OD. An intelligent non-uniform mixing of red and green channels is introduced for denoising of retinal photographs because of the dissimilar noise level in each channel. Template based matching technique is applied for OD localization of retinal image. The approach is thoroughly verified on openly accessible the DRIVE and the STARE datasets for OD detection and denoising of retinal images. This denoising technique greatly improved the accuracy of OD detection in contrast to other contending approaches.

Keywords: Retina Images, STARE, Optic Disc, template matching, DRIVE

1 Introduction

The digital fundus photographs are broadly utilized for timely identification of various retinal abnormalities [1]. The main factor of vision damage and completely loss of sight in the working population is because of major retinal disorders e.g. glaucoma and Diabetic Retinopathy (DR) [2]. Timely identification of such abnormalities by screening programs and subsequently medication can forestall vision loss [3]. The fundamental step for CAD system is the automatic diagnoses and investigation of retinal photographs for these ailments. The variation in physical structure of human eye is an indicator for these abnormalities. The identification of retinal structure which contains: blood vessel network, OD, optic cup, macula and fovea are a significant precondition to detect retinal disorders automatically [1].

OD is considered very imperative element for glaucoma recognition and different lesions evaluation associated with DR [4]. The significant structural arrangements present in the retinal photograph are displayed in Fig. 1. The blood vessels and Optic Nerves Head (ONH) emerge in the OD of retina. OD is called blind part as it containing no light-detecting cells. The healthy retinal photographs have the yellowish brightest OD region and it resembling to almost circular oval disk. Accurate OD recognition is an elementary stride for CAD system of various ophthalmic abnormalities, for instance DR and glaucoma [5]. The variation in OD structure can estimate the level of blindness and its different characteristics can be utilized to identify visual syndromes. The characteristics like, breadth and boundary of cup, mean cup depth, range of OD, rim part and Cup-Disc-Ratio (CDR) are commonly used to diagnose glaucoma [6]. The detection and extraction of other anatomical shapes e.g. fovea, macula and retinal blood vessels can be easier, once OD is localized [7]. Furthermore, ocular abnormalities of the retinal vasculature can be observed in various diseases such as hypertension, stroke, diabetes and glaucoma [3]. Surplus of insulin in the blood is a source of progressive ocular disorder called

DR which can damage vision if not observed timely [8]. Micro-vascular problem of diabetes also initiated DR, which is treated one of the major source of vision loss. DR is considered one of the actual causes of visual impairment in developed states by numerous literature [9]. Hypertensive retinopathy occurs because of high blood pressure [10]. The presence of arteriovenous scratching is a remarkable indication of stroke [11]. OD recognition is initial step to scrutinize glaucoma, which is worldwide the second leading source of vision loss [12].

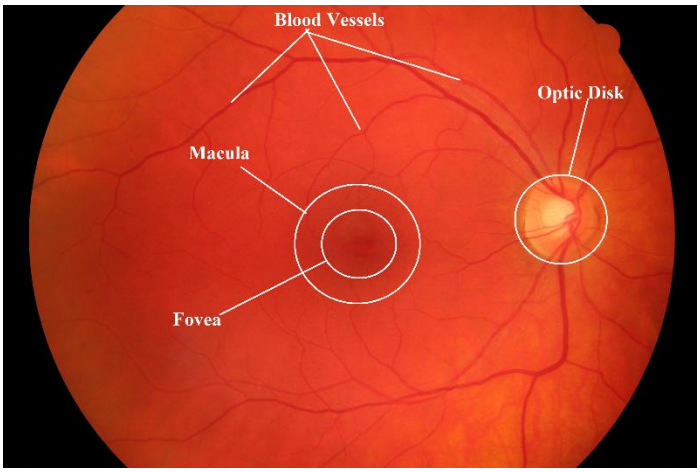

Fig. 1. Anatomical structure of the retinal image.

Glaucoma is brought about by the expansion in the intraocular fluid density in the ONH, as a result of either obstruction or a greater creation of aqueous humor of the eye [1]. Glaucoma stays asymptomatic at an initial period and gradually increases which eventually prompts visual deficiency. Medication is only successful at the initial phases because once the ONH dented can't be treated [13]. The initial occurrence of glaucoma can be recognized by detection and extraction of the OD and optic cup, proceeded by calculating the CDR. The physical variations in OD provide serious evidences relating to glaucoma diagnosis [14]. A CAD framework is essential for huge population based scrutiny of glaucoma. OD recognition and extraction is the fundamental move towards the advancement of CAD. Recognizing the importance of such frameworks, a few OD algorithms have been suggested and endeavored by numerous, however it's still a dynamic exploration zone.

OD extraction is a hard task because of the dissimilarities in its structure, dimension, and color and also there are several others difficulties to be considered. Generally, there is contrast variation all around the OD border. Another problem is the eye blinking at the time of capturing fundus image can obscured photographs, causing their automatic investigation even harder. This issue can be addressed by just disposing such photographs and recapturing new ones. Conversely, this approach is not generally used as their quality is generally adequate for human pictorial examination.

This framework endeavors to identify the OD in fundus photographs by suppressing noise. The associated literature is discussed in section II, the designed model is clarified in section III and the experimental analysis and conclusion is elaborated in section IV and V, respectively.

2 Review of the Literature

Numerous techniques were recommended by researchers for OD recognition and boundary extraction. Sinthanayothin et al. [15], suggested a technique to extract the position of the OD by identifying the region in the photograph, which has the maximum intensity deviation. As the OD often seems as a bright disc, the difference in pixel illumination is maximum there. This method stated a precision of 99.1% on 112 photographs for identification of the OD position. In low contrast RGB retinal photographs, the OD detection is achieved by coupling of a Hausdorff-based template matching approach on edge map lead by pyramidal decomposition for enormous scale elements tracing [16]. Lowell [17], detected the OD position by a template matching scheme and dissection by a deformable contour model in low contrast images. Foracchia et al. [18], employed a geometrical parametric model for localization of the OD. Xu et al. [19], suggested an innovative deformable model based technique for automatic localization of OD borderline in the fundus photographs. They refined and extended the original snake method in two aspects: clustering and smoothing update. Niemeijer et al. [20], extracted the anatomical structures by fitting a single point-distribution-model. The framework employs a cost function depend on the coupling of both global and local cues, to search the accurate location of the model points. Another method [21], is proposed to extract the OD position based on matching the retinal vasculature. The image is first normalized by adaptive histogram equalization, then matched filter is employed to approximately match the track of vessels at the OD locality. Reza et al. [22], preprocessed the retinal image for the OD and exudates detection by utilizing average filtering, contrast enhancement, and thresholding. Further, morphological operators, extended maxima/minima operator and watershed transformation were used. In [23], a novel adaptive technique is proposed based on mathematical morphology for detection of the OD in digital retinal photographs. Aquino et al. [24], designed a framework for OD localization utilizing morphological and boundary extraction algorithms followed by the Circular Hough Transform (CHT). In [25], recognition of the OD and exudates on low resolution photographs are obtained by Digital Curvelet Transform (DCT) and level set approach. This method doesn't need any human intervention and is vigorous to the contrast variation in the retinal photographs. Qureshi et al. [26], proposed a combination of pyramidal decomposition entropy measure, edge detection, and Hough transformation techniques to identify the OD. Another method [27], suggested a histogram matching technique for detection of the OD. Pereira et al. [28], proposed Ant Colony Optimization (ACO) for the features extraction followed by anisotropic diffusion for the extraction of the OD. In [29], Approximate Nearest Neighbour Field (ANNF) and Feature match approach is suggested to locate the relationship

between a selected OD reference photograph and any given input photograph. Basit and Fraz [30], proposed the OD detection technique utilizing morphological & smoothing filters and watershed transformation. Another framework [31], employed pixel intensities and candidate-based technique for detection of the OD. Dashtbozorg et al. [32], proposed a framework for OD localization employing a multiresolution Sliding Band Filter (SBF). Nimbarte and Mushrif [33], designed a histon-based approach for the localization of the OD, in which roughness index of the histon and histogram is employed for thresholding. Xiong and Li [34], proposed a three stages methodology: Region-Of-Interest (ROI) recognition, candidate pixel identification, and confidence score computation for the OD localization. Abdullah et al. [35], suggested a combination of morphological filters, the CHT and the grow-cut method for the extraction of the OD. The retinal vessels network and other abnormalities are eradicated by morphological operators along with enhancement of the OD. The OD midpoint is estimated utilizing the CHT, and the grow-cut method is engaged to accurately extract the OD borderline.

3 Proposed Method

3.1 Overview

In the proposed approach, denoising of retina images and OD identification is attained by utilizing non-uniform channels mixing and template based matching, respectively. Most important concern of this study is to minimize the noise in the retinal images. A common issue in OD detection is the noise which seems as illuminated bright spots on the boundaries of the retinal photographs. The input RGB retinal image is splitted into RED, GREEN and BLUE bands. The visual inspection of red band clearly indicates the effect of fringe noise is very less on the boundaries as compared to the green channel. Fig. 2 indicates step-wise representation of the proposed methodology.

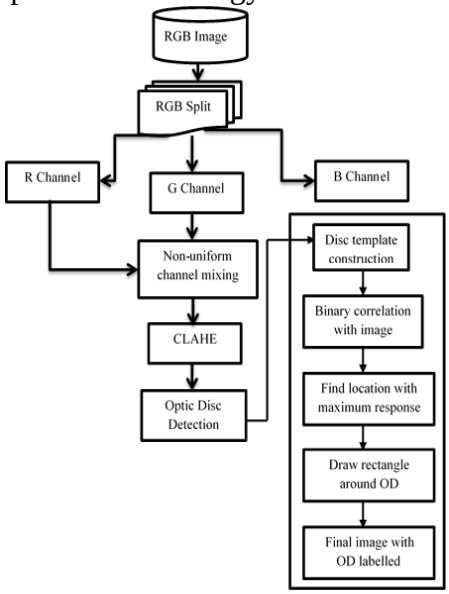

Fig. 2. Block diagram of the proposed approach.

3.2 Denoising and contrast enhancement of the retina image

1. Green channel is non-uniformly fused with the red channel. Referring to Fig. 3, green channel have a prominent contrast among background, vessel pixels and geometrical objects e.g. OD, macula etc. But it contained fringe noise on the edges. To suppress fringe noise effect, a non-uniform mixing of green channel with red channel is performed. The visual analysis indicates that fringe noise have less effect on the edges of red band of the retina photograph. The edges of red band is highly prioritized while mixing with the green channel and the rest of the part of the red channel is mixed in such manner to add minor effect on the green channel. In this way, the noise suppression is achieved while maintaining a prominent contrast between background and vessel pixels of the green channel.

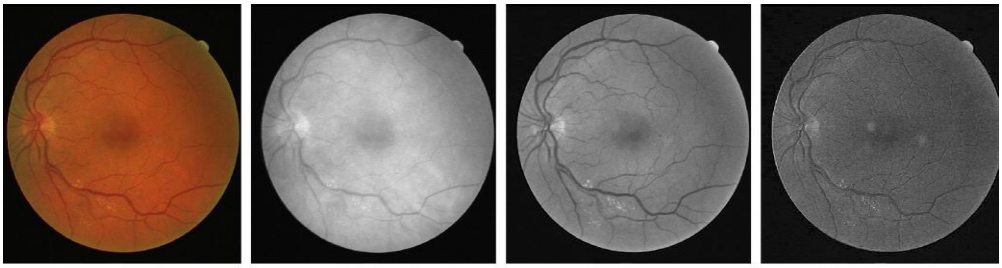

Fig 3. Retinal color photograph and its channels pictorial valuation. (a) RGB input photograph (b) Red channel (c) Green channel (d) Blue channel

2. The Contrast Limited Adaptive Histogram Equalization (CLAHE) is further utilized to perform local contrast enhancement. The vessels and geometrical objects are enhanced and becomes more prominent after the application of the CLAHE.
3. Morphological filters are applied to remove blood vessels, macula, fovea and background noise.
4. The OD is detected and segmented according to the steps shown in Fig.2.
5. Finally, a denoised image with accurate detection of OD and boundary segmentation is obtained.

3.3 Template Construction for OD extraction

The identification of OD is the preliminary stage of numerous vessel extraction and disease screening systems. The way of constructing template is defined in [27]. In order to identify the midpoint of the OD, a mean filter with the kernel of 6×6 is used on the retina photograph to diminish the influence of noise. Then, the complete retina photograph is scanned with the template of size 81×81 pixels. In each window under the sliding template, the RGB channels are isolated and their histogram

is computed individually. Then, the correlation between the histogram of each band in the sliding window and the histograms of its parallel band in the template is computed. The cross-correlation function is used to find the resemblance of the two histograms; though, the identified OD midpoints are not exact by utilizing these procedures. The function CX utilized for computing correlation is represented as following:

$$\boldsymbol{CX} = \frac{\mathbf{1}}{(\mathbf{1} + \sum_{\boldsymbol{i}}(\boldsymbol{m_i} - \boldsymbol{n_i})^{\mathbf{2}})} \tag{1}$$

where m and n are two histograms that are used to determine their correlation. Therefore, if m and n are similar $\sum_{\boldsymbol{i}}(\boldsymbol{m_i} - \boldsymbol{n_i})^{\mathbf{2}} \approx 0$, and Corr ≈ 1, else and Corr << 1. Consequently, equation (1) can be used to compute the correlation between two histograms and the outcome of correlation is lies between 0 and 1.

Each time with sliding window, three values are obtained as the consequences of correlation between the histograms. The outcome of histograms similarity is calculated as the weighted sum of the three attained values:

$$\boldsymbol{CX}\,(\boldsymbol{k}, \boldsymbol{l}) = \boldsymbol{w_r} \times \boldsymbol{CX_r} + \boldsymbol{w_g} \times \boldsymbol{CX_g} + \boldsymbol{w_b} \times \boldsymbol{CX_b} \tag{2}$$

where $(\boldsymbol{k}, \boldsymbol{l})$ is the middle of sliding window. $\boldsymbol{CX_r}$,$\boldsymbol{CX_g}$ and $\boldsymbol{CX_b}$ are the outcomes of correlation for three channels and $\boldsymbol{w_r}$, $\boldsymbol{w_g}$, and $\boldsymbol{w_b}$ are the weights of each band. In equation (2), different weights can be used for $\boldsymbol{CX_r}$, $\boldsymbol{CX_g}$ and $\boldsymbol{CX_b}$. The peak weight is assigned to the green band due to its higher contrast than the other two channels [36]. In various fundus photographs, blue band is noisy; therefore, to reduce the influence of blue band, we define the lowest weight for blue band. The suitable weights $\boldsymbol{w_r} = \mathbf{0.5}$,$\boldsymbol{w_g} = \mathbf{2}$ and $\boldsymbol{w_b} = \mathbf{1}$ are selected through experimental results for accurate recognition of OD. To identify the midpoint of OD, thresholding is applied on the correlation function $\boldsymbol{CX}\,(\boldsymbol{k}, \boldsymbol{l})$.

For optimum selection of threshold, a comprehensive scanning of various values is performed and the suitable relation to search the threshold is found in equation (3).

$$\boldsymbol{Threshold} = \mathbf{0.5} * \mathbf{max}(\boldsymbol{CX}) \tag{3}$$

4 Results and Analysis

The proposed scheme has been verified on freely obtainable datasets DRIVE [37], STARE [38], DIARETDB0 and DIARETDB1 [39], which contains both normal and abnormal images. The validation has been performed on 40 fundus photographs from the DRIVE dataset, 81 fundus photographs from the STARE dataset, 110 fundus photographs from a DIARETDB0 dataset, and 89 fundus photographs from

a DIARETDB1 dataset. The precision rate is 100%, 97.53%, 97.27%, and 97.75% for the DRIVE, STARE, DIARETDB0, and DIARETDB1 datasets, correspondingly.

The step-by-step visual illustration of the proposed approach is exposed in Fig.4. In Table 1, the visual results of the proposed scheme for some fundus photographs from the DRIVE and STARE databases are displayed. The histogram assessment of the OD is more effective in the manifestation of anomaly in the eye. Abnormal segments, exudates and OD are bright areas in the retina photographs. Hence, the segmentation results of blood vessels are unsuccessful to identify the midpoint of the OD in presence of abnormal segments and exudates in the retina photograph.

Table 1 indicates visual analysis of the proposed method scheme on both normal and abnormal retina images. The outcomes of the proposed scheme are acceptable in the presence of dark hemorrhages or bright exudates and abnormal segments and it shows the efficiency of the proposed scheme for detecting the midpoint of OD. In Table 1, some fundus photographs with wrongly spotted OD midpoint are displayed.

In the STARE dataset case, in some images there is no vasculature in neighborhood of OD and the properties of OD-like illumination and excessive quantity of vessels in locality of OD cannot be observed; therefore, the proposed scheme is unsuccessful to detect the OD midpoint. Therefore, in situation like the second image of STARE dataset in Table 1 that we have abnormal segments with large vessel network, the proposed scheme is unable to find midpoint of OD.

TABLE I. Visual performance assessment of the DRIVE and STARE Dataset

DRIVE Dataset Images	STARE Dataset Images
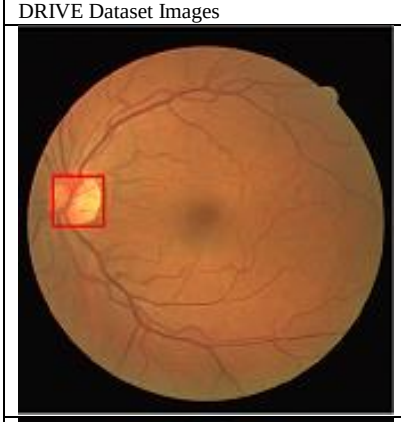	
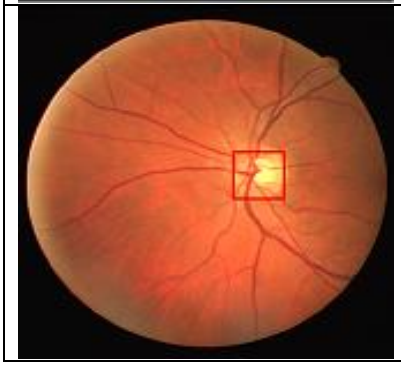	

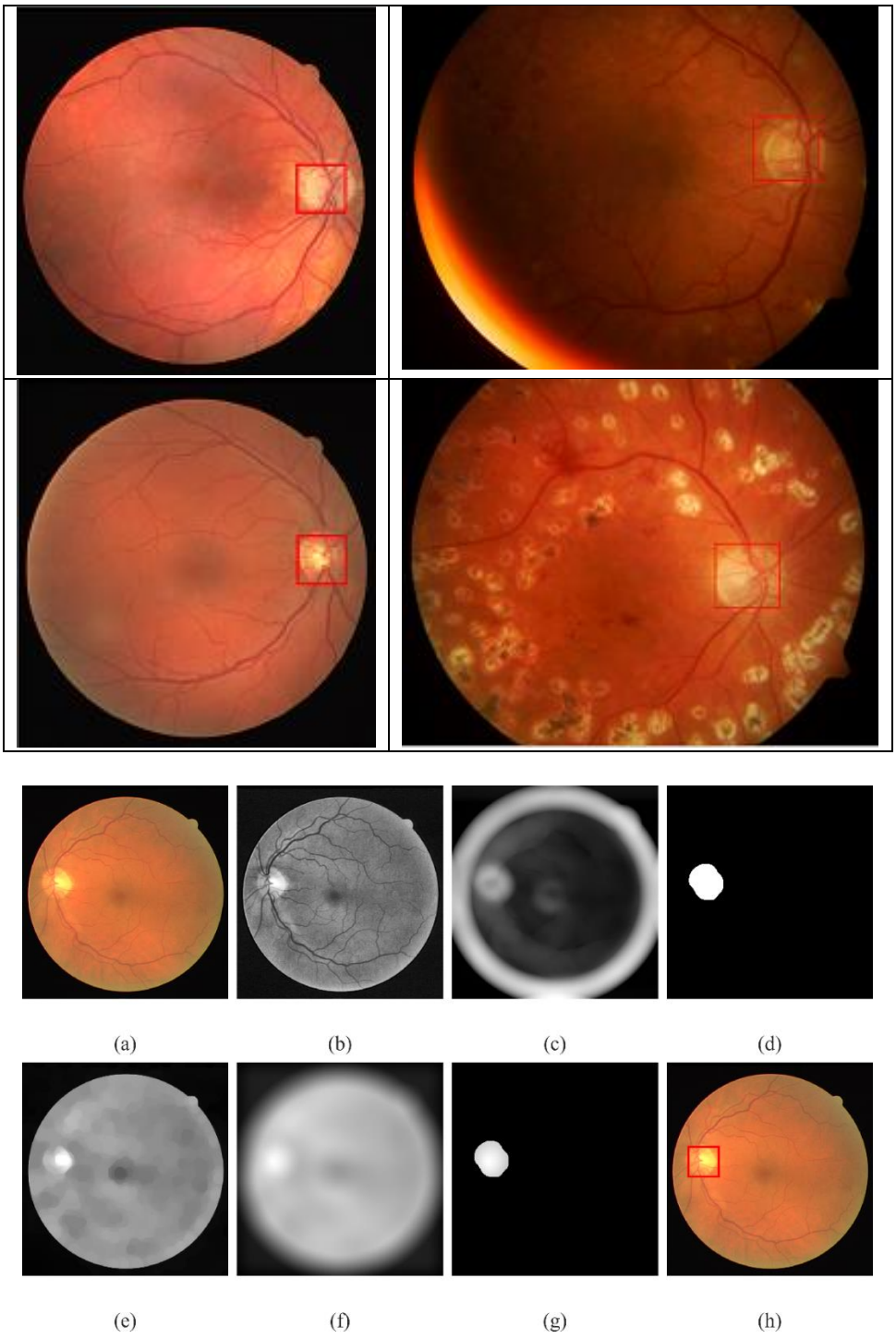

Fig. 4. Pictographic demonstration of the proposed scheme (a) RGB image from DRIVE dataset (b) Green and Red band non-uniform channel mixing and contrast enhancement, (c) Application of morphological operators for geometrical objects removal, (d) Template creation, (e) Morphological operations, (f) Template matching (correlation), (g) Find location, (h) OD detected and drawn rectangle.

The proposed methodology performances is tested on various datasets as shown in Table II. Comparison of the proposed method and other existing approaches is shown in Table III, which validates the efficiency of the proposed scheme. The databases utilized for validation of the proposed scheme containing a larger number of images than the databases utilized in other competing techniques. To escape the preprocessing steps such as segmentation, the proposed scheme bears less computation complexity in comparison to the counterpart methods. In techniques that utilize segmentation required a great number of processes per pixel and resultantly increase the computation time. The proposed scheme is fast as we avoid the preprocessing steps such as segmentation.

TABLE II. Performance measure of the OD identification of different datasets

DRIVE			
No. of Images	**OD detected**	**OD missed**	**Result (%)**
40	40	0	100
DIARETDB0			
No. of Images	**OD detected**	**OD missed**	**Result (%)**
110	107	3	97.27
STARE			
No. of Images	**OD detected**	**OD missed**	**Result (%)**
81	79	2	97.53
DIARETDB1			
No. of Images	**OD detected**	**OD missed**	**Result (%)**
89	87	2	97.75

TABLE III. Comparison with other OD detection approaches

Technique	**Year**	**Dataset**	**Result Accuracy (%)**
Foracchia et al. [18]	2004	STARE	98
Niemeijer et al. [20]	2009	LOCAL	91
Youssif et al. [21]	2008	DRIVE	100
		STARE	98.8
Welfer et al. [23]	2010	DRIVE	100
		DIARETDB1	97.7
Aquino et al. [24]	2010	MESSIDOR	99
Esmaeili et al. [25]	2012	DRIVE	100
		STARE	93.8
		DIARETDB1	100
Qureshi et al. [26]	2012	DRIVE	100
		DIARETDB0	96.8

TABLE III. (Continued): Comparison with other OD detection approaches

		DIARETDB1	94.02
		DRIVE	100
Dehghani et al. [27]	2012	STARE	91.4
		LOCAL	98.9
Pereira et al. [28]	2013	DRIVE	100
		DIARETDB1	93.3
		DRIVE	100
		STARE	93.9
Ramakanth [29]	2014	DIARETDB0	98.5
		DIARETDB1	98.9
		MESSIDOR	99.42
		DRIVE	100
Basit and Fraz [30]	2015	DIARETDB1	98.9
		CHASE_DB1	100
		DRIVE	97.5
Ahmed [31]	2015	DIARETDB1	86.5
		VICAVR	93.1
		MESSIDOR	97.8
Nimbarte [33]	2016	DRIVE	95
		DIARETDB1	91
		DRIVE	100
Xiong and Li [34]	2016	STARE	95.8
		DIARETDB0	99.2
		DIARETDB1	97.8
		DRIVE	100
Proposed	2018	STARE	97.53
		DIARETDB0	97.27
		DIARETDB1	97.75

5 Conclusion

The statistical and visual results endorses that the proposed system achieves considerably better performance than many other recent OD localization methods. The OD localization consequences evidently represent the capability of the proposed scheme to detect OD in the presence of abnormalities which may increase the probabilities of false positives. Moreover, the system produced good results on the photographs with uneven brightness and abnormal segments.

References

[1] J.J. Kanski, B. Bowling, *Clinical Ophthalmology: A Systematic Approach*, Elsevier Health Sciences, 2011.

[2] K.B. Khan, A.A. Khaliq, M. Shahid and S. Khan, An efficient technique for retinal vessel segmentation and denoising using modified ISODATA and CLAHE, *IIUM Engineering Journal*, **17** (2016), no. 2, 31-46.

[3] M. Fraz, P. Remagnino, A. Hoppe, B. Uyyanonvara, A.R. Rudnicka, C.G. Owen, S.A. Barman, Blood vessel segmentation methodologies in retinal images - a survey, *Comput. Methods Programs Biomed.*, **108** (2012), no. 1, 407-433. https://doi.org/10.1016/j.cmpb.2012.03.009

[4] M. Niemeijer, M. D. Abramoff and B. van Ginneken, Segmentation of the optic disc, macula, and vascular arch in fundus photographs, *IEEE Trans. Med. Imaging*., **26** (2007), no. 1, 116-127. https://doi.org/10.1109/tmi.2006.885336

[5] KB. Khan, A.A. Khaliq and M. Shahid, A Novel Fast GLM Approach for Retinal Vascular Segmentation and Denoising, *Journal of Information Science and Engineering*, **33** (2017), no. 6, 1611-1627.

[6] H. Li, O. Chutatape, A model-based approach for automated feature extraction in fundus images, *Proceedings. Ninth IEEE International Conference on Computer Vision*, (2003), 394-399. https://doi.org/10.1109/iccv.2003.1238371

[7] L. Xiong, H. Li, An approach to locate optic disc in retinal images with pathological changes, *Computerized Medical Imaging and Graphics*, **47** (2016), 40-50. https://doi.org/10.1016/j.compmedimag.2015.10.003

[8] R. Klein, B.E. Klein, S.E. Moss, Visual impairment in diabetes, *Ophthalmology*, **91** (1984), no. 1, 1-9. https://doi.org/10.1016/s0161-6420(84)34337-8

[9] A.K. Sjølie, J. Stephenson, S. Aldington, E. Kohner, H. Janka, L. Stevens, J. Fuller, EURODIAB IDDM Complications Study Group. Retinopathy and vision loss in insulin-dependent diabetes in Europe: the EURODIAB IDDM Complications Study, *Ophthalmology*, **104** (1997), no. 2, 252-260.

[10] C. Heneghan, J. Flynn, M. O'Keefe, M. Cahill, Characterization of changes in blood vessel width and tortuosity in retinopathy of prematurity using image analysis, *Medical Image Analysis*, **6** (2002), no. 4, 407-429. https://doi.org/10.1016/s1361-8415(02)00058-0

[11] J. Lowell, A. Hunter, D. Steel, A. Basu, R. Ryder, R. L. Kennedy, Measurement of retinal vessel widths from fundus images based on 2-D modeling, *IEEE Transactions on Medical Imaging*, **23** (2004), no. 10, 1196-1204. https://doi.org/10.1109/tmi.2004.830524

[12] H. A. Quigley, A.T. Broman, The number of people with glaucoma worldwide in 2010 and 2020, *British Journal of Ophthalmology*, **90** (2006), no. 3, 262-267. https://doi.org/10.1136/bjo.2005.081224

[13] R. N. Weinreb, T. Aung, F. A. Medeiros, The pathophysiology and treatment of glaucoma: a review, *JAMA*, **311** (2014), no. 18, 1901-1911. https://doi.org/10.1001/jama.2014.3192

[14] M.D. Abràmoff, M.K. Garvin, M. Sonka, Retinal imaging and image analysis, *IEEE Reviews in Biomedical Engineering*, **3** (2010), 169-208. https://doi.org/10.1109/rbme.2010.2084567

[15] C. Sinthanayothin, J. F. Boyce, H. L. Cook, T. H. Williamson, Automated localisation of the optic disc, fovea, and retinal blood vessels from digital colour fundus images, *British Journal of Ophthalmology*, **83** (1999), no. 8, 902-910. https://doi.org/10.1136/bjo.83.8.902

[16] M. Lalonde, M. Beaulieu, L. Gagnon, Fast and robust optic disc detection using pyramidal decomposition and Hausdorff-based template matching, *IEEE Transactions on Medical Imaging*, **20** (2001), no. 11, 1193-1200. https://doi.org/10.1109/42.963823

[17] J. Lowell, A. Hunter, D. Steel, A. Basu, R. Ryder, E. Fletcher, L. Kennedy, Optic nerve head segmentation, *IEEE Transactions on Medical Imaging*, **23** (2004), no. 2, 256-264. https://doi.org/10.1109/tmi.2003.823261

[18] M. Foracchia, E. Grisan, A. Ruggeri, Detection of optic disc in retinal images by means of a geometrical model of vessel structure, *IEEE Transactions on Medical Imaging*, **23** (2004), no. 10, 1189-1195. https://doi.org/10.1109/tmi.2004.829331

[19] J. Xu, O. Chutatape, P. Chew, Automated optic disk boundary detection by modified active contour model, *IEEE Transactions on Biomedical Engineering*, **54** (2007), no. 3, 473-482. https://doi.org/10.1109/tbme.2006.888831

[20] M. Niemeijer, M. D. Abràmoff, B. Van Ginneken, Fast detection of the optic disc and fovea in color fundus photographs, *Medical Image Analysis*, **13** (2009), no. 6, 859-870. https://doi.org/10.1016/j.media.2009.08.003

[21] A. A. Youssif, A. Z. Ghalwash, A. A. Ghoneim, Optic disc detection from normalized digital fundus images by means of a vessels' direction matched filter, *IEEE Transactions on Medical Imaging*, **27** (2008), no. 1, 11-18. https://doi.org/10.1109/tmi.2007.900326

[22] A. W Reza, C. Eswaran, S. Hati, Automatic tracing of optic disc and exudates from color fundus images using fixed and variable thresholds, *Journal of Medical Systems*, **33** (2009), no. 1, 73-80. https://doi.org/10.1007/s10916-008-9166-4

[23] D. Welfer, J. Scharcanski, C. M. Kitamura, M.M. Dal Pizzol, L. W. Ludwig, D. R. Marinho, Segmentation of the optic disk in color eye fundus images using an adaptive morphological approach, *Computers in Biology and Medicine*, **40** (2010), no. 2, 124-137. https://doi.org/10.1016/j.compbiomed.2009.11.009

[24] A. Aquino, M. E. Gegúndez-Arias, D. Marín, Detecting the optic disc boundary in digital fundus images using morphological, edge detection, and feature extraction techniques, *IEEE Transactions on Medical Imaging*, **29** (2010), no. 11, 1860-1869. https://doi.org/10.1109/tmi.2010.2053042

[25] M. Esmaeili, H. Rabbani, A. M. Dehnavi, A. Dehghani, Automatic detection of exudates and optic disk in retinal images using curvelet transform, *IET Image Processing*, **6** (2012), no. 7, 1005-1013. https://doi.org/10.1049/iet-ipr.2011.0333

[26] R. J. Qureshi, L. Kovacs, B. Harangi, B. Nagy, T. Peto, A. Hajdu, Combining algorithms for automatic detection of optic disc and macula in fundus images, *Computer Vision and Image Understanding*, **116** (2012), no. 1, 138-145. https://doi.org/10.1016/j.cviu.2011.09.001

[27] A. Dehghani, H. A. Moghaddam, M. S. Moin, Optic disc localization in retinal images using histogram matching, *EURASIP Journal on Image and Video Processing*, **2012** (2012), no. 1, 19. https://doi.org/10.1186/1687-5281-2012-19

[28] C. Pereira, L. Gonçalves, M. Ferreira, Optic disc detection in color fundus images using ant colony optimization, *Medical & Biological Engineering & Computing*, **51** (2013), no. 3, 295-303. https://doi.org/10.1007/s11517-012-0994-5

[29] S. A. Ramakanth, R. V. Babu, Approximate nearest neighbour field based optic disk detection, *Computerized Medical Imaging and Graphics*, **38** (2014), no. 1, 49-56. https://doi.org/10.1016/j.compmedimag.2013.10.007

[30] A. Basit, M. M. Fraz, Optic disc detection and boundary extraction in retinal images, *Applied Optics*, **54** (2015), no. 11, 3440-3447. https://doi.org/10.1364/ao.54.003440

[31] M. I. Ahmed, M. A. Amin, High speed detection of optical disc in retinal fundus image, *Signal, Image and Video Processing*, **9** (2015), no. 1, 77-85. https://doi.org/10.1007/s11760-012-0412-3

[32] B. Dashtbozorg, A. M. Mendonça, A. Campilho, Optic disc segmentation using the sliding band filter, *Computers in Biology and Medicine*, **56** (2015), 1-12. https://doi.org/10.1016/j.compbiomed.2014.10.009

[33] N. Nimbarte, M. Mushrif, Extraction of blood vessels and optic disc in retinal images, *Computer Methods in Biomechanics and Biomedical Engineering: Imaging & Visualization*, **6** (2018), no. 1, 31-42. https://doi.org/10.1080/21681163.2016.1154806

[34] L. Xiong, H. Li, An approach to locate optic disc in retinal images with pathological changes, *Computerized Medical Imaging and Graphics*, **47** (2016), 40-50. https://doi.org/10.1016/j.compmedimag.2015.10.003

[35] M. Abdullah, M. M. Fraz, S. A. Barman, Localization and segmentation of optic disc in retinal images using circular Hough transform and grow-cut algorithm, *PeerJ*, **4** (2016), e2003. https://doi.org/10.7717/peerj.2003

[36] A. Osareh, B. Shadgar, Automatic blood vessel segmentation in color images of retina, *Iranian Journal of Science and Technology*, **33** (2009), no. B2, 191.

[37] J. Staal, M. D. Abràmoff, M. Niemeijer, M. A. Viergever, B. Van Ginneken, Ridge-based vessel segmentation in color images of the retina, *IEEE Transactions on Medical Imaging*, **23** (2004), no. 4, 501-509. https://doi.org/10.1109/tmi.2004.825627

[38] A. D. Hoover, V. Kouznetsova, M. Goldbaum, Locating blood vessels in retinal images by piecewise threshold probing of a matched filter response, *IEEE Transactions on Medical Imaging*, **19** (2000), no. 3, 203-210. https://doi.org/10.1109/42.845178

[39] http://www.it.lut.fi/project/imageret/diaretdb1/#DOWNLOAD

Received: April 28, 2018; Published: June 4, 2018